Journal of Naval Architecture and Marine Engineering
January, 2026
https://dx.doi.org/10.3329/jname.v23i1.73805 *https://www.banglajol.info*

HEAT TRANSFER ANALYSIS ON FERROMAGNETIC HYBRID NANOFLUID DYNAMICS WITH THE EFFECT OF THERMAL RADIATION AND INDUCED MAGNETIC FIELD

T.R. Krishnaveni[1], B. Srinivasa Kumar[2], G.V. Ramana Reddy[3]

[1]Research Scholar, Department of Mathematics, Koneru Lakshmaiah Education Foundation, Vaddeswaram, Guntur (Dt), India-522302. Email: radhaphd.18@gmail.com

[2]Department of Mathematics, Koneru Lakshmaiah Education Foundation, Vaddeswaram, Guntur (Dt), India-522302, Email: sk_bhavirisetty@kluniversity.in

[3]Department of Mathematics, Koneru Lakshmaiah Education Foundation, Vaddeswaram, Guntur (Dt), India-522302, Email: gvrr1976@gmail.com

Abstract:

By clarifying the impact of thermal radiation and induced magnetisms, this study explains the heat transformation analysis on ferromagnetic hybrid nano fluid dynamics. When heat transfer occurs in the presence of generated heat within the boundary layer, the induced magnetic field is taken into account. Heat generation and fluid thermal analysis are thought to be important within the boundary layer (BL) in order to standardize the dynamics process. PDEs, or partial differential equations, are used to describe the model. Ordinary differential equations (ODEs) are a further transformation of PDEs. The set of ODEs has been investigated using the spectrum relaxation method (SRM). The SRM is an iterative method for solving differential equations that makes use of the Gauss-seidel technique notion. It is observed that a higher Prandtl number causes the velocity and temperature to decrease. The thickness of the momentum BL is significantly influenced by the induced magnetic field. Together with thermal BL thickness, it was found that heat generation and thermal radiation increased momentum. Applications of this research can be found in the automotive and thermal engineering sectors. It is observed that the new analysis concurs with earlier publications.

Keywords: Heat transfer, ferromagnetic nanofluid, thermal radiation, induced magnetic field, boundary layer, spectral relaxation method.

NOMENCLATURE

u_1, u_2	velocity components
H_1^*, H_2^*	parallel and normal portion of the induced magnetic field
Kis	Boltzman constant
T	Fluid temperature
Qis	Heat generation
H_e^*	Free stream magnetic field
q_r	heat flux
c_p	heat capacity at constant pressure
T_w, T_∞	free and ambient temperature of wall

Greek Symbols

ρ	fluid density
υ_{hnf}	Kinematic viscosity of hybrid nano fluid
η_0	magnetic viscosity
α_{hnf}	Thermal diffusivity of hybrid nanofluid

1. Introduction

In research, induced magnetic field considerations have drawn the attention of numerous scholars. The external magnetic field produces induced magnetism. Vertebral currents are created when electrons circulate due to this external magnetic field. Applications include thermal engineering MHD accelerators, magnetic materials, and plasma. Numerous writers have studied metals that resemble ferromagnets and contain atoms that behave like tiny magnets. The application of recently induced magnetic fields resulting from ferromagnetic hybrid-nanofluid dynamics of heat and mass transfer was investigated by Li et al. (2024). We simultaneously examined the impact

1813-8535 (Print), 2070-8998 (Online) Received: June, 2024

of inductive magnetism (Dolui et al., 2023). In tandem with heat radiation, ternary hybrid nanofluids are flowing. The impact of gradient magnetic characteristics on the dynamics of chemically reactive hybrid nanofluids was examined by Arshad et al. (2023). The thermal and mass permeation characteristics of magnetic dipoles in hybrid-Kasson-nanofluid dynamics were examined by Ahmad et al. (2021). Beyond the permeating bent stretch/reduced surface, the impact of Lorentz forces, which are defined by induced magnetism, is significant for Casson's micro polar nanofluid dynamics according to Amjad et al. (2020). The effects of induced magnetic currents are examined by Bashir et al. (2021) in conjunction with the theoretical theory of Kalau-Yasda nanofluid dynamics. The thermal process of nanoparticular dynamics is significantly influenced by thermal radiation. Thermal radiation and heat generation are highly useful in industrial and heat operations. Many scientists have used technical applications to draw attention to the literature regarding the testing of thermal radiation and heat output. Ali et al. (2021) investigated the effects of thermal radiation in addition to non-uniform heat flow on MHD hybrid nanofluids in the direction of elastic cylinders.

Masood et al. (2021) observed how heat absorption and generation, along with stagnation points, affect the behavior of polystyrene-TIO2/H2O hybrid nanofluids. Hussain et al. (2021) studied MHD hybrid nanofluids in areas where there is thermal radiation. Shah et al. (2022) focused on thermal radiation and how entropy is produced in hybrid nanofluids. They also looked into the movement of hybrid nanofluids. Alhussain et al. (2021) explored ways to improve thermal conductivity and magnetic bio induction within nanofluid systems. Ahmad et al. (2021) discussed how Maxwell-hybrid nanofluids can improve thermal efficiency on stretchable surfaces. Yan et al. (2021) studied the Xue and Maxwell models for hybrid nanofluid films on tilted moving surfaces. Wei-Feng et al. (2022) examined nonlinear mixed convection in hybrid nanofluids with various slip edge conditions. Zubair et al (2021) observed how thermal radiation impacts MHD analysis in porous panes within Darcy-Forchheimer models of hybrid nanofluids. Sadiq et al. (2021) explained the effects of radiation and Soret on ethylene glycol water based on the dynamics of Maxwell Nanofluid in upright channels. Muhammad et al. (2021) investigated the boundary layer MHD dynamics of Darcy-Forchheimer Radiation Nanofluid. Jena et al. (2018) investigated the chemical reactions to MHD viscoelastic fluid dynamics after vertical stretchy leaves with heat source/decreased. Laza et al. (2023) investigated the role of nanostrips on trihybrid nanofluid flow on double permeable hard disks. Khaled et al. (2023) examined models of Fourier heat sources and Fourier heat flow for sexually hybrid nanofluids via hard drives. Khatun and Nasrin (2021) examined numerical modelling of Bouonqiornos Nanofluid for free convection: thermophobia and brown effects. Ali et al. (2021) investigated the analysis of nanofluid flows in boundary layers on the surface of elastic, permeable wedge-shaped with magnetic effects.

Zahan et al. (2019) Mixed convection hybrid nanofluid flow examined by lid velocity: Effects of MHD and Joule heating. Ahmed et al. (2018) delved into the mesmerizing world of natural convection currents in circular and arc-shaped chambers infused with water-based nanofluids. In a separate exploration, Falodun et al. (2024) unraveled the intricate numerical simulations of antibacterial and antiviral strategies employing Casson-Walter-B fluids and silver nanoparticles, focusing on the dynamics of fluctuating thermophysical characteristics. A thorough survey of existing literature unveils a plethora of investigations centered on hybrid nanofluids, particularly those rich in MnZnFe2O4 and Fe2O4 compositions. This research zeroes in on the analysis of heat transfer within ferromagnetic hybrid nanofluid dynamics, influenced by magnetic fields and the phenomenon of thermal radiation. The ensuing assumptions serve to enhance the framework of this innovative study:

(i) Ferromagnetic hybrid nanofluids made of MnZnFe2O4 and Fe2O4 were studied.
(ii) Heat generation and thermal radiation are considered important factors in the flow.
(iii) The study also looked at induced magnetic fields and how thermal radiation affects these ferromagnetic nanofluids. So far, no research has looked into how heat transfer works in these nanofluids when considering both thermal radiation and induced magnetic fields, based on the literature reviewed here.

To fill this gap, it is important to study how magnetic and thermal forces together affect the rate of heat transfer, the stability of the liquid, and how particles are distributed in the fluid. This study provides deeper insight into the optimization of ferromagnetic hybrid nanofluids for advanced heat transfer applications and lays the basis for improving thermal management solutions in a variety of technologies and technical fields.

2. Mathematical Analysis

Assuming a laminar, steady and incompressible hybrid nanofluid dynamics past a stretchable surface. The content of the hybrid nanofluid are taken to be $MnZnFe_2O_4$ and Fe_2O_4 while engine oil is considered to be the base fluid.

The velocity at the free stream is taking to be $u_e^* = ax$ while at the wall where $a, c > 0$ the velocity is taken to be $u_w(x) = cx$. In this research, the magnetism Reynolds number is considered to be high, and the induced magnetism field is assumed to be significant. The concentration along with temperature towards the wall are C_w and T_w while free stream concentration along with temperature are C_∞ and T_∞ respectively. All fluid properties remain constant and considering the boundary layer approximations to obtain the governing equations are formed as

$$\frac{\partial u_1}{\partial x} + \frac{\partial u_2}{\partial y} = 0 \tag{1}$$

$$\frac{\partial H_1^*}{\partial x} + \frac{\partial H_2^*}{\partial y} = 0 \tag{2}$$

$$u_1 \frac{\partial u_1}{\partial x} + u_2 \frac{\partial u_1}{\partial y} - \frac{\mu_e^*}{4\rho_{hnf}\pi}\left(H_1^* \frac{\partial H_1^*}{\partial x} + H_2^* \frac{\partial H_1^*}{\partial y}\right) = u_e^* \frac{du_e^*}{dx} - \frac{\mu_e^* H_e^*}{4\rho_{hnf}\pi}\frac{dH_e^*}{dx} + \nu_{hnf}\frac{\partial^2 u_1}{\partial y^2} - \frac{\mu_{hnf}}{K}u_1 \tag{3}$$

$$u_1 \frac{\partial H_1^*}{\partial x} + u_2 \frac{\partial H_1^*}{\partial y} = H_1^* \frac{\partial u_1}{\partial x} + H_2^* \frac{\partial u_1}{\partial y} + \eta_0 \frac{\partial^2 H_1^*}{\partial y^2} \tag{4}$$

$$u_1 \frac{\partial T}{\partial x} + u_2 \frac{\partial T}{\partial y} = \alpha_{hnf}\frac{\partial^2 T}{\partial y^2} + \frac{Q}{\rho c_p}(T - T_\infty) - \frac{1}{(\rho c_p)_{hnf}}\frac{\partial q_r}{\partial y} \tag{5}$$

Subject to the boundary conditions as follows:

$$u_1 = u_w(x) = cx,\ v = 0,\ \frac{\partial H_1^*}{\partial y} = H_2^* = 0,\ T = T_w\ at \quad y = 0 \tag{6}$$

$$u_2 = u_e^* = ax,\ H_1^* = H_e^*,\ T = T_\infty\ \text{as} \quad y \longrightarrow \infty \tag{7}$$

In this context, u_1 and u_2 represent the velocity components, α stands for thermal diffusivity, x and y are the coordinates, H_1^* and H_2^* are the induced magnetism vectors, k is the Boltzmann constant, T is temperature, η_0 is the magnetic diffusivity, ν is the kinematic viscosity, μ_e^* is the magnetic permeability, H_e^* represents the free stream magnetic fields, and T_∞ is the free stream temperature.

The heat flux is simplified by implementing the Rosseland diffusion process as employed in Reddy et al. (2022) as:

$$q_r = -\frac{4\sigma_s}{3k_e}\frac{\partial T^4}{\partial y} \tag{8}$$

σ_s signifies the Stefan-Boltzmann constant while k_e signifies coefficient of mean absorption. The difference in temperature in fluid dynamics is taken to be small in other to express T^4 as a linear function by simplifying T^4 about T_∞ by implementing Taylor's series and ignoring higher terms to given

$$T^4 \cong 4T_\infty^3 T - 3T_\infty^4 \tag{9}$$

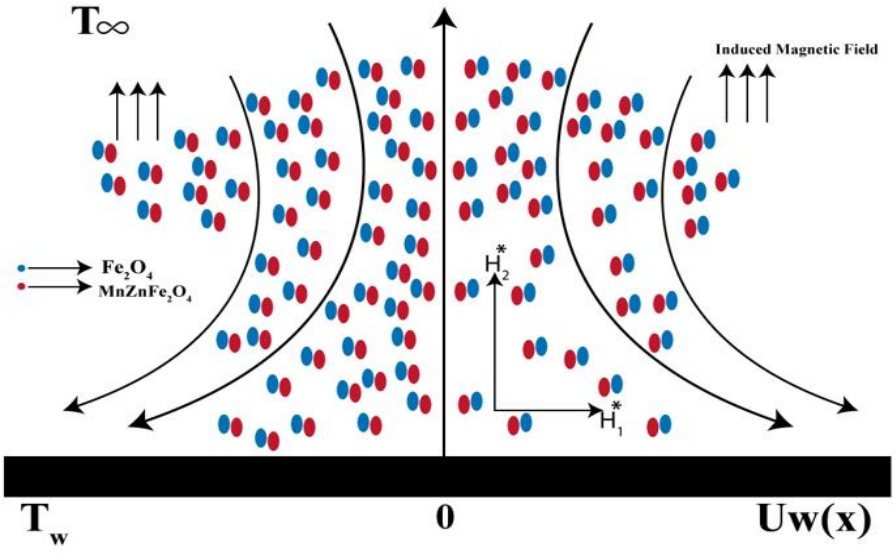

Figure 1: Physical configuration of the model

The similarity transformation variables are defined as follows:

$$u_1 = xcf'(\eta), u_2 = -f(\eta)\sqrt{\nu_f c}, \eta = y\sqrt{\frac{c}{\nu_f}}, H_1^* = H_0\left(\frac{x}{l}\right)g'(\eta), H_2^* = -g(\eta)H_0\sqrt{\frac{\nu_f}{l^2 c}},\ \theta = \frac{T - T_\infty}{T_w - T_\infty}, \tag{10}$$

Based on the above and use of the similarity transformations to obtain

$$\frac{1}{\omega_1}f''' + \omega_2(ff'' - (f')^2 + (A^*)^2) + M((g')^2 - gg'' - 1) - \frac{1}{Po}f' = 0 \quad (11)$$

$$\lambda^* g''' + g''f - gf'' = 0 \quad (12)$$

$$\frac{K_{hnf}}{K_f}\left(\frac{1+R}{Pr}\right)\theta'' + \omega_3(f\theta' + Qo\theta) = 0 \quad (13)$$

The nondimesional boundary conditions as follows:

$f = 0,\ \ f' = 1,\ \ g = 0,\ \ g'' = 0,\ \ \theta = 1,\ at\ \eta = 0$ and

$$f' = A^*, g' = 1, \theta = 0\ as\ \eta \to \infty \quad (14)$$

The controlled parameters as defined in the transformed equations are $A^* = \frac{a}{c}$ is velocity ratio parameter, $M = \frac{\mu_e^* H_0^2}{4\pi c^2 l^2 \rho_f}$ is a magnetism parameter, $\lambda^* = \frac{\eta_0}{\nu_f}$ is the reciprocal of the magnetism Prandtl number, $Pr = \frac{\nu_f}{\alpha_f}$ is Prandtl number, $Re_x = \frac{xu_w}{\nu_f}$ is local Reynolds number, $R = \frac{4\sigma_0 T_\infty^3}{3kek^*}$ is the thermal radiation parameter, $P_0 = \frac{\rho ck}{\mu^*}$ is the permeability term, $Q_0 = \frac{Q}{c\rho c_p}$ is the heat generation term. It should be noted that ω_1, ω_2 and ω_3 are defined as: $\omega_1 = (1-\varphi_1)^{2.5}(1-\varphi_2)^{2.5}$, $\omega_2 = \left\{(1-\varphi_2)[(1-\varphi_1) + \frac{\varphi_1\rho_{s1}}{\rho_f}]\right\} + \frac{\varphi_2\rho_{s2}}{\rho_f}$, $\omega_3 = \left\{(1-\varphi_2)[(1-\varphi_1) + \frac{\varphi_1(\rho c_p)_{s1}}{(\rho c_p)_f}]\right\} + \frac{\varphi_2(\rho c_p)_{s2}}{(\rho c_p)_f}$. It should be noted that ω_1, ω_2 and ω_3 represent the thermophysical properties of the hybrid nanofluid.

Table 1: Thermophysical features of hybrid nano fluid (see Li et al. (2024));

Property	Symbol	Mathematical expression
Density	ρ	$\rho_{hnf} = \{(1-\varphi_2)[\rho_f(1-\varphi_1) + \rho_{s1}\varphi_1]\} + \varphi_2\rho_{s2}$
Dynamic viscosity	μ	$\mu_{hnf} = \frac{\mu_f(1-\varphi_2)^{-2.5}}{(1-\varphi_1)^{2.5}}$
Thermal conductivity	k	$\frac{k_{hnf}}{k_{nf}} = \frac{k_{s_2} + 2k_{nf} - 2\varphi_1(k_{nf} - k_{s_2})}{k_{s_2} + 2k_{nf} + \varphi_2(k_{nf} - k_{s_2})}$ $\frac{k_{nf}}{k_f} = \frac{k_{s_1} + 2k_f - 2\varphi_1(k_f - k_{s_1})}{k_{s_1} + 2k_f + \varphi_1(k_f - k_{s_1})}$
Heat capacity	ρc_p	$(\rho c_p)_{hnf} = \{(1-\varphi_2)[(\rho c_p)_f(1-\varphi_1) + (\rho c_p)_{f_{s1}}\varphi_1]\} + \varphi_2(\rho c_p)_{f_{s2}}$

Table 2: Thermophysical characteristics of water, engine oil, Fe_2O_4 and $MnZnFe_2O_4$ (see Li et al. (2024))

Symbol	Water	Engine oil (Unused at 360K)	Fe_2O_4	$MnZnFe_2O_4$
ρ	997.1	847.8	5180	4700
c_p	4179	2161	670	1050
k	0.613	0.138	9.7	3.9
P_r	6.3	30	---	---

3. Methodology (Spectral relaxation method)

This section explains the basic steps of the spectral relaxation method which is employed in solving the transformed ODEs (11)-(13). To implement the SRM, the technique of the Gauss-Sediel approach is used to obtain the linear equations in (17)-(19). The Gauss-seidel approach is capable of decoupling and linearizing differential equations. The decoupled and linearized equations are iteratively discretized by obtaining the linear terms within $r+1$ current iteration level while all nonlinear terms at r previous iteration level. By implementing the SRM, the following equations are obtained:

$$\frac{1}{\omega_1}f'''_{r+1} + \omega_2 f_r f''_{r+1} - \omega_2(f'_{r+1})^2 + \omega_2(A^*)^2 + \beta^*(g'_r)^2 - \beta^* g_r g''_r - \beta^* - \frac{1}{Po}f'_{r+1} = 0 \quad (14)$$

$$\frac{K_{hnf}}{K_f}\left(\frac{1+R}{Pr}\right)\theta''_{r+1} + \omega_3 f_{r+1}\theta'_{r+1} + \omega_3 Qo\theta_{r+1} = 0 \quad (15)$$

$$\lambda^* g'''_{r+1} + f_{r+1}g''_{r+1} - g_{r+1}f''_r = 0 \quad (16)$$

In other to linearize and decompose the equations, the coefficient parameters are:

$$a_{0,r} = \omega_2 f_r, \qquad a_{1,r} = -\omega_2 (f'_{r+1})^2, \qquad a_{2,r} = -\beta^* \omega_2 (A^*)^2, \qquad a_{3,r} = -\beta^* g_r g''_r, \qquad a_{4,r} = \beta^* (g'_r)^2$$

$$b_{0,r} = \frac{K_{hnf}}{K_f}\left(\frac{1+R}{Pr}\right), \; b_{1,r} = \omega_3 f_{r+1}, \; b_{2,r} = \omega_3 Qo,$$

Substituting the coefficient parameters above to obtain:

$$\frac{1}{\omega_1} f'''_{r+1} + a_{0,r} f''_{r+1} + a_{1,r} + a_{2,r} + a_{4,r} + a_{3,r} - \frac{1}{Po} f'_{r+1} = 0 \tag{17}$$

$$b_{0,r} \theta''_{r+1} + b_{1,r} \theta'_{r+1} + b_{2,r} \theta_{r+1} = 0 \tag{18}$$

$$\lambda^* g'''_{r+1} + c_{0,r} g''_{r+1} - c_{1,r} g_{r+1} = 0 \tag{19}$$

The interpolating function of Chebyshev polynomials is defined over the Gauss-Lobatto collocation points which is defined as:

$$\xi_j = cos\frac{\pi j}{N}, \quad j = 0,1,2,\dots,N, \quad -1 \le \xi \ge 1$$

Where the numeric collocation point is N. To further implement the SRM, the original domain of $[0,\infty)$ is completely changed into $[-1,1]$ by implementing the procedures of domain truncation. Hence, the solution to the current problem is gotten at $[0,L]$ and not $[0,\infty)$. The mapping function is hereby defined as

$$\eta = \left(\frac{\xi+1}{2}\right)L, \qquad -1 \le \xi \ge 1$$

Finaly, the solution to the problem is computed iteratively until it yields a convergency and a level of accuracy is reached. Due to the spectral method's exponential convergence rate, SRM can achieve very high accuracy with relatively few iterations compared to traditional finite difference or finite element methods. By linearizing nonlinearity iteratively, SRM avoids directly solving complex nonlinear systems at each step, making it more computationally efficient.

4. Results and Discussion

The outcomes from the numerical simulation are discussed in this section. The significant impact of dynamics parameters is presented graphically while the impact on engineering quantities of interest is tabulated. The numerical simulations of dynamics parameters are conducted implementing the spectral relaxation method. The detailed explanation of this numerical scheme has been discussed in the previous section. The control terms are permeability parameter (P_o), inverse of magnetic Prandtl number (λ^*), thermal radiation (R), Prandtl number (Pr), heat generation (Qo) and magnetic parameter (M). The values of these terms are chosen based on experimental computations, hence $P_o = 1.0, \lambda^* = 0.81, \; R = 0.5, Pr = 0.71, Qo = 2.0$ and $M = 1.0$.

Figure 2 shows the significant of M on the velocity and induced velocity contour. An upsurge in the magnitude of M elevates magnetism forces within the boundary layer. A higher M was found to degenerate the f' and g' profiles respectively. This is a result of the magnetic force such as force of Lorentz which drags the dynamics of an electrically assisting fluid. This outcome in Figure 2 is in concord with MHD principles which explains that a higher value of magnetic fields reduces the motion of a conducting fluid in the heat transfer process. Figure 3 illustrates the significant impact of Po within the boundary layer. The permeability regime allows the passage of fluid particles from one regime to another within the boundary layer. Increasing the magnitude of Po will hereby increase the random collision of nanofluid particles. Hence, the momentum boundary layer thickness increases due to the increased value of Po.

Figure 4 shows how Pr affects the temperature pattern. When Pr increases, the temperature profile becomes less intense. Because Pr represents low thermal conductivity, it causes the thermal boundary layer to become thinner and the fluid temperature to drop. In real terms, a higher Pr means less ability to conduct heat. Figure 5 shows how the heat generation term (Qo) influences both the velocity and temperature patterns. Heat generation happens when energy from chemical, electrical, or nuclear sources turns into heat. This process improves the thermal condition of the ferromagnetic nanoparticles. In Figure 5, when Qo increases, both the fluid temperature and velocity increased. Figure 6 shows how thermal radiation affects the velocity and temperature patterns. Increasing R leads to higher temperatures within the boundary layer. A larger R value causes more random collisions, which heat up the fluid nanoparticles, making both the thermal and momentum boundary layers thicker.

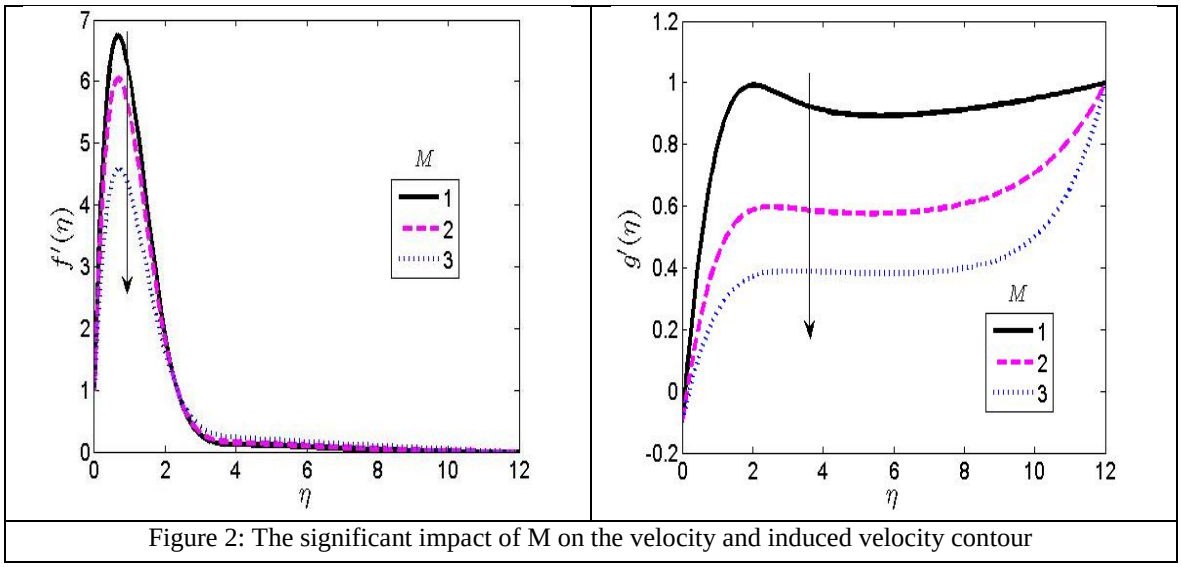

Figure 2: The significant impact of M on the velocity and induced velocity contour

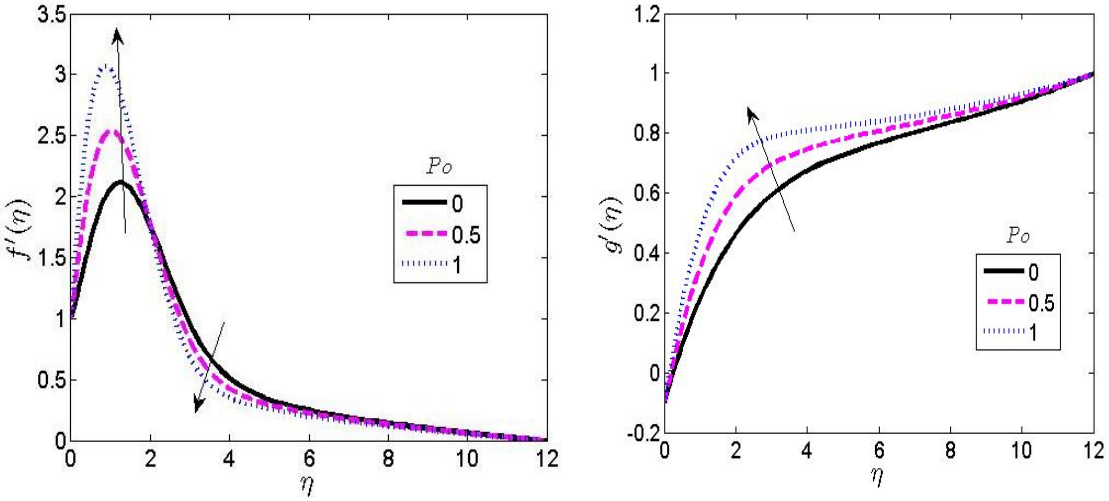

Figure 3: The significant impact of Po on the velocity and induced velocity contours.

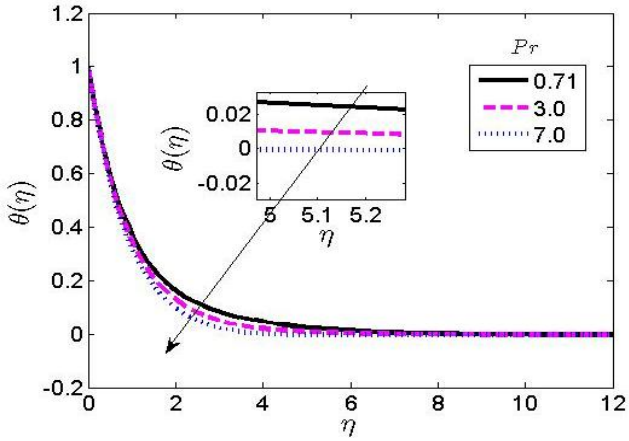

Figure 4: The significant impact of Pr on the temperature contour

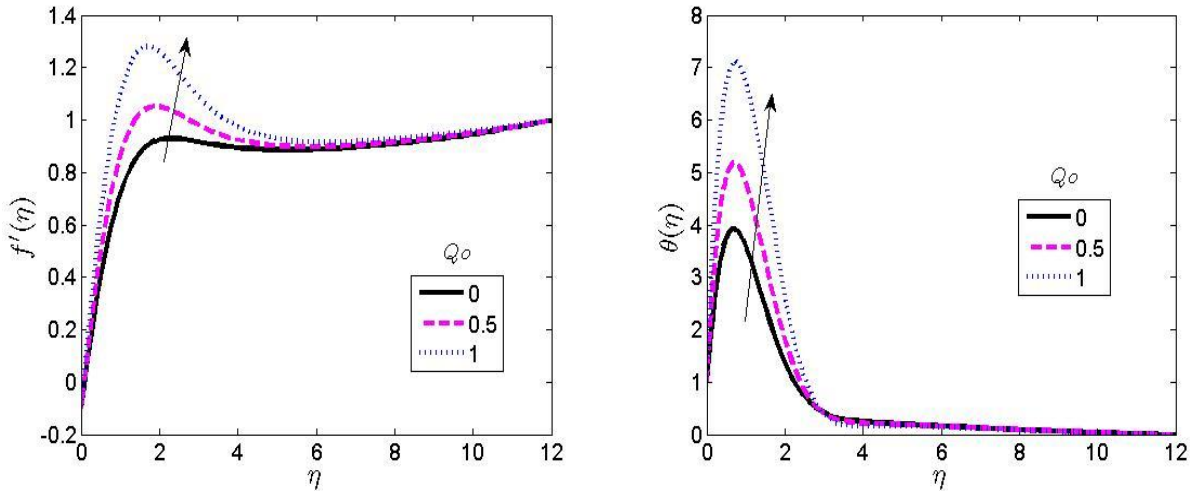

Figure 5: The significant impact of Qo on the velocity and temperature contours.

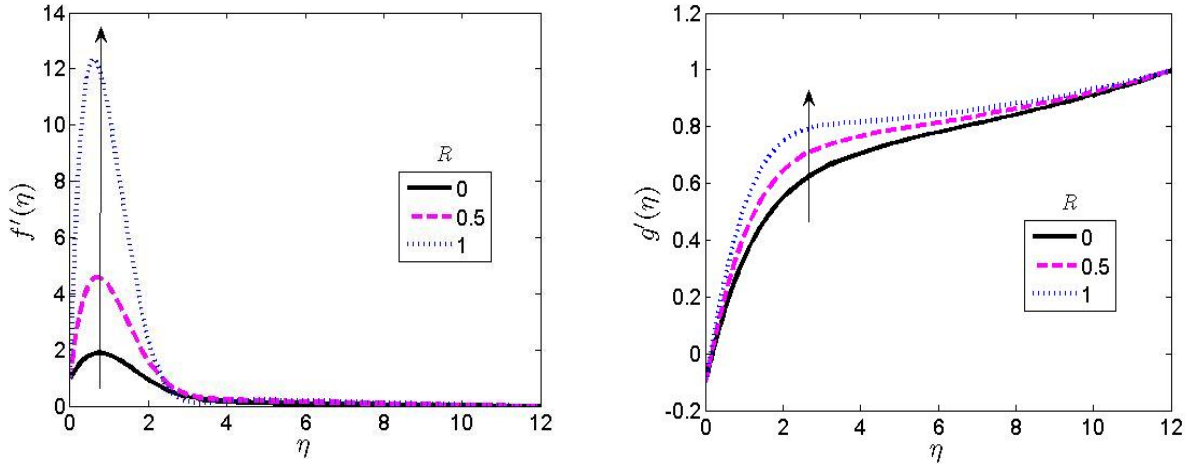

Figure 6: The significant impact of R on the velocity and temperature contours

5. Conclusion

This study looked into how heat moves through a special kind of fluid made with magnetic nanoparticles, considering the effect of a magnetic field and heat radiation. The equations that describe this process were changed and then solved using a method called SRM. SRM was used to solve these modified equations step by step. The study shows how different factors affecting the flow are clearly shown in graphs. The main results of this research are listed as follows:

(i) When the magnetic field strength increases, it creates stronger magnetic forces that pull and slow down the movement of a conducting electrically charged fluid.
(ii) If the permeability parameter is higher, it causes the fluid to flow more quickly and the particles in the boundary layer to collide more randomly.
(iii) Increasing both thermal radiation and heat generation causes the temperature to rise and makes the thermal boundary layer thicker.
(iv) It was found that a higher value of the Prandtl number results in lower thermal conductivity, which in turn reduces the temperature of the fluid.

Acknowledgements

The authors are grateful to the Department of Mathematics, Koneru Lakshmaiah Education Foundation, Vaddeswaram, Guntur (Dt), for their valuable support while preparing the manuscript.

References

Ahmad, F., Abdal, S., Ayed, H., Hussain, S., Salim, S., and Almatroud, A. O. (2021). The improved thermal efficiency of Maxwell hybrid nanofluid comprising of graphene oxide plus silver/kerosene oil over stretching sheet. Case Studies in Thermal Engineering, 27, 101257. https://doi.org/10.1016/j.csite.2021.101257

Ahmed, K. F. U., Nasrin, R. and Elias, M. (2018). Natural convective flow in circular and arc cavities filled with water-cu nanofluid: A comparative study, Journal of Naval Architecture and Marine Engineering, 15, 37-52, https://doi.org/10.3329/jname.v15i1.33549

Ahmad, S., Khan, M. N., Rehman, A., Felemban, B. F., Alqurashi, M. S., Alharbi, F. M., Alotaibi, F. and Galal, A. M. (2021). Analysis of heat and mass transfer features of hybrid Casson nanofluid flow with the magnetic dipole past a stretched cylinder. Applied Sciences, 11(23), 11203. https://doi.org/10.3390/app112311203

Alhussain, Z. A., Renuka, A., and Muth Tamilselvan, M. (2021). A magneto-bioconvective and thermal conductivity enhancement in nanofluid flow containing gyrotactic microorganism. Case Studies in Thermal Engineering, 23, 100809. https://doi.org/10.1016/j.csite.2020.100809

Ali, A., Kanwal, T., Awais, M., Shah, Z., Kumam, P., and Thounthong, P. (2021). Impact of thermal radiation and non-uniform heat flux on MHD hybrid nanofluid along a stretching cylinder. Scientific reports, 11(1), 20262. https://doi.org/10.1038/s41598-021-99800-0

Amjad, M., Zehra, I., Nadeem, S., Abbas, N., Saleem, A., and Issakhov, A. (2020). Influence of Lorentz force and induced magnetic field effects on Casson micropolar nanofluid flow over a permeable curved stretching/shrinking surface under the stagnation region. Surfaces and Interfaces, 21, 100766.https://doi.org/10.1016/j.surfin.2020.100766

Arshad, M., Alharbi, F. M., Hassan, A., Haider, Q., Alhushaybari, A., Eldin, S. M., and Galal, A. M. (2023). Effect of inclined magnetic field on radiative heat and mass transfer in chemically reactive hybrid nanofluid flow due to dual stretching. Scientific Reports, 13(1), 7828.https://doi.org/10.1038/s41598-023-34871-9

Bashir, S., Ramzan, M., Chung, J. D., Chu, Y. M., and Kadry, S. (2021). Analyzing the impact of induced magnetic flux and Fourier's and Fick's theories on the Carreau-Yasuda nanofluid flow. Scientific Reports, 11(1), 9230.https://doi.org/10.1038/s41598-021-87831-6

Dolui, S., Bhaumik, B., and De, S. (2023). Combined effect of induced magnetic field and thermal radiation on ternary hybrid nanofluid flow through an inclined catheterized artery with multiple stenosis. Chemical Physics Letters, 811, 140209. https://doi.org/10.1016/j.cplett.2023.140756

Falodun, B. O., Tijani, M. O., Adenekan, I. O., Abraham, O. A., and Ogunsanya, T. I. (2025). Numerical simulation of antibacterial and antiviral mechanisms using silver nanoparticles with the dynamics of Casson-Walters-B and variable thermophysical properties. World Journal of Engineering, 22(4), 699–710. https://doi.org/10.1108/WJE-11-2023-0494

Hussain, A., Hassan, A., Al Mdallal, Q., Ahmad, H., Rehman, A., Altanji, M., and Arshad, M. (2021). Heat transport investigation of magneto-hydrodynamics (SWCNT-MWCNT) hybrid nanofluid under the thermal radiation regime. Case Studies in Thermal Engineering, 27, 101244. https://doi.org/10.1016/j.csite.2021.101244

Jena, S., Dash, G.C., Mishra, S.R. (2018) Chemical reaction effect on MHD viscoelastic fluid flow over a vertical stretching sheet with heat source/sink, Ain Shams Engineering Journal 9,1205-1213, https://doi.org/10.1016/j.asej.2016.06.014

Khaled, A., Alharbi, K. A. M., Farooq, U., Noreen, S., Imran, M., Akgül, A., Kanani, M., Asad, J. (2023). Numerical approach toward ternary hybrid nanofluid flow with nonlinear heat source-sink and fourier heat flux model passing through a disk, InternationalJournalofThermofluids18, 100367. https://doi.org/10.1016/j.ijft.2023.100367

Li, S., Saadeh, R., Madhukesh, J. K., Khan, U., Ramesh, G. K., Zaib, A., Prasannakumara, B.C., Kumar, R., Ishak, A. and Sherif, E. S. M. (2024). Aspects of an induced magnetic field utilization for heat and mass transfer ferromagnetic hybrid nanofluid flow driven by pollutant concentration. Case Studies in Thermal Engineering, 53, 103892. https://doi.org/10.1016/j.csite.2023.103892

Mahmood, Z., Eldin, S. M., Rafique, K., and Khan, U. (2023). Numerical analysis of MHD trihybrid nanofluid over a nonlinear stretching/shrinking sheet with heat generation/absorption and slip conditions. Alexandria Engineering Journal, 76, 799-819. https://doi.org/10.1016/j.aej.2023.06.081

M. Ali, R. Nasrin, M. A. Alim, (2021), Analysis of boundary layer nanofluid flow over a stretching permeable wedge-shaped surface with magnetic effect, journal of Naval Architecture and Marine Engineering, 18, 11-24. https://doi.org/10.3329/jname.v18i1.44458

Masood, S., Farooq, M., and Anjum, A. (2021). Influence of heat generation/absorption and stagnation point on polystyrene-TiO2/H2O hybrid nanofluid flow. Scientific Reports, 11(1), 22381. https://doi.org/10.1038/s41598-021-01747-9

Muhammad, J,. Khan, A., Saeed, A., Kumam, P., Shah, Z. (2021). Analysis of boundary layer MHD Darcy-Forchheimer radiative nanofluid flow with Soret and Dufour effects by means of Marangoni convection, Case Studies in Thermal Engineering 23, 100792. https://doi.org/10.1016/j.csite.2020.100792

Qadeer, R., Wang, X., Siddique, I., Ali, B., Eldin, S. M., Yang, H. (2023). Role of nanolayer on the dynamics of tri-hybrid nanofluid subject to gyrotactic microorganisms and nanoparticles morphology vis two porous disks, Case Studies in Thermal Engineering 51, 103534. https://doi.org/10.1016/j.csite.2023.103534

Sadiq, K., Jarad, F., Siddique, I., and Ali, B. (2021). Soret and radiation effects on mixture of ethylene glycol-water (50%-50%) based Maxwell nanofluid flow in an upright channel. Complexity, 1-12. https://doi.org/10.1155/2021/5927070

Shagaiya, D. Y., Aziz, Z. A., Ismail, Z., Salah, F. (2018). Impact of thermal radiation on electrical MHD f low of nanofluid over nonlinear stretching sheet with variable thickness, Alexandria Engineering Journal 57, 2187-2197. https://doi.org/10.1016/j.aej.2017.07.007

Shah, N.S.M.R., Liu, D., Muhammad, T., Waqas, H., Eldin, S. M., Yasmin, S., Khan, A. S. (2022). Numerical simulations of hybrid nanofluid flow with thermal radiation and entropy generation effects, Case Studies in Thermal Engineering 40, 102479. https://doi.org/10.1016/j.csite.2022.102479

Khatun, S. and Nasrin, R. (2021). Numerical modelling of Buongiorno's nanofluid on free convection thermophoresis Brownian effects, Journal of Naval Architecture and Marine Engineering, 18, 217-239. https://doi.org/10.3329/jname.v18i2.54694

Wei-Feng, X., Ahmad, S., Khan, M.N., Ahmad, H., Rehman, A., Baili, J., Gia, T.N. (2022). Heat and mass transfer analysis of nonlinear mixed convective hybrid nanofluid flow with multiple slip boundary conditions, Case Studies in Thermal Engineering, 32, 101893. https://doi.org/10.1016/j.csite.2022.101893

Yan, Z., Shahmir, N., Ramzan, M., Ghazwani, H. A. S., Malik, M.Y. (2021). Comparative analysis of Maxwell and Xue models for a hybrid nanofluid film flow on an inclined moving substrate, Case Studies in Thermal Engineering 28, 101598. https://doi.org/10.1016/j.csite.2021.101598

Zahan, I., Nasrin, R., and Alim, M.A. (2019). Mixed convective hybrid nanofluid flow in lid-driven undulated cavity: Effect of MHD and Joule heating, Journal of Naval Architecture and Marine Engineering, 16(2019) 109-126. https://doi.org/10.3329/jname.v16i2.40585

Zubair, M., Jawad, M., Bonyah, E., and Jan, R. (2021). MHD analysis of couple stress hybrid nanofluid free stream over a spinning Darcy-Forchheimer porous disc under the effect of thermal radiation. Journal of Applied Mathematics, 1-18. https://doi.org/10.1155/2021/2522155